Available online at www.sciencedirect.com
SCIENCE DIRECT®
Journal of Organometallic Chemistry 689 (2004) 2837–2844
Journal of Organometallic Chemistry
www.elsevier.com/locate/jorganchem

Oxalate-bridged dirhenium(I) hexacarbonyl complexes: synthesis, reactions, and crystal structures

Rui Zhang [a], Chee Leong Kee [a], Weng Kee Leong [b], Yaw Kai Yan [a,*]

[a] *Natural Sciences Academic Group, National Institute of Education, Nanyang Technological University, NIE Blk 7 Science, 1 Nanyang Walk, Singapore 637616, Republic of Singapore*

[b] *Department of Chemistry, National University of Singapore, 3 Science Drive 3, Singapore 117543, Republic of Singapore*

Received 25 May 2004; accepted 3 June 2004
Available online 7 July 2004

Abstract

The complex $[\{Re(CO)_5\}_2(\mu,\eta^1{:}\eta^1\text{-}C_2O_4)]$ **1** undergoes thermal decarbonylation to give $[Re_2(CO)_6(C_2O_4)]_n$, which reacts with triphenylphosphine and *trans*-1,2-bis(diphenylphosphino)ethylene (dppene) to give *anti*-$[Re_2(PPh_3)_2(CO)_6(\mu,\eta^2{:}\eta^2\text{-}C_2O_4)]$ **2** and $[Re_2(\mu\text{-dppene})(CO)_6(\mu,\eta^2{:}\eta^2\text{-}C_2O_4)]$ **4**, respectively. Complex **2** is oxidized on prolonged exposure to air (1 week) to form *anti*-$[Re_2(OPPh_3)_2(CO)_6(\mu,\eta^2{:}\eta^2\text{-}C_2O_4)]$ **3**. In the presence of excess dppene, the complex $[Re_2(\mu\text{-dppene})_2(CO)_6(\mu,\eta^1{:}\eta^1\text{-}C_2O_4)]$ **5** is also formed alongside **4**. With the chelating diphosphine 1,3-bis(diphenylphosphino)propane (dppp), the complex $[(\eta^2\text{-dppp})Re(CO)_3(\mu,\eta^1{:}\eta^1\text{-}C_2O_4)Re(CO)_3(\eta^2\text{-dppp})]$ **6** is formed. The structures of **3** and **4** have been determined by X-ray crystallography. The dppene ligand in complex **4** adopts an unusual "*syn*" conformation wherein the two phosphorus lone pairs of electrons are eclipsed, thus forming an "A-frame" type of bridge.

Keywords: Rhenium; Carbonyl; Carboxylate; Oxalate; Phosphine; *trans*-1,2-Bis(diphenylphosphino)ethylene

1. Introduction

Rhenium (I) carbonyl carboxylato complexes have not been extensively studied [1–5]. This is especially the case for complexes containing bridging dicarboxylate ligands. There is virtually no data on the synthesis and properties of dicarboxylate-bridged dirhenium (I) carbonyl complexes, the only reported example of such a complex being $[\{Re(CO)_5\}_2(\mu,\eta^1{:}\eta^1\text{-}C_2O_4)]$ **1**, which was synthesised by the reaction of $[Re(CO)_5BF_4]$ with oxalic acid in aqueous solution [4]. There is apparently no further study of the chemistry of complex **1**.

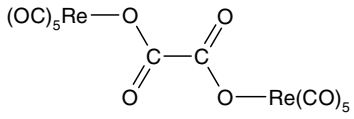

1

There is much current interest in the development of radiopharmaceuticals through the radiolabeling of monoclonal antibodies with ^{188}Re for the treatment of cancer (radioimmunotherapy) [6–9]. The ability of antibodies to recognize epitopes on tumour cells gives a basis for targeted delivery of radioactivity to malignant tumours. Although much emphasis had been placed on the development of ligand systems for chelation to the Re(V) oxo core [7], the design of radiopharmaceuticals based on the Re(I)-tricarbonyl moiety has gained considerable attention recently [8,9].

* Corresponding author. Tel.: +65-6-790-3374; fax: +65-6-896-9432.
E-mail address: ykyan@nie.edu.sg (Y.K. Yan).

0022-328X/$ - see front matter © 2004 Elsevier B.V. All rights reserved.
doi:10.1016/j.jorganchem.2004.06.017

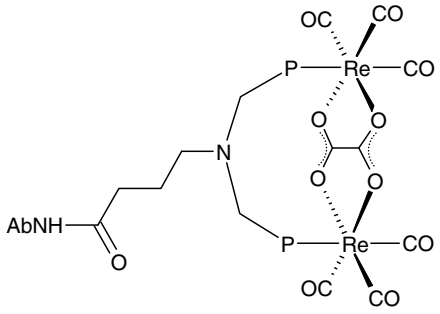

Fig. 1. Attachment of a bis(bidentate)-oxalate-bridged dirhenium(I) hexacarbonyl unit to an antibody ($AbNH_2$) via a carboxyl-functionalized diphosphine.

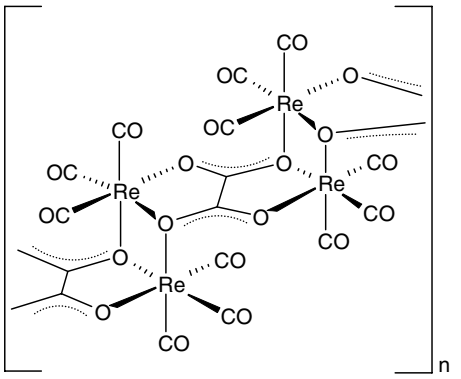

Fig. 2. Proposed structure of $[Re_2(CO)_6(C_2O_4)]_n$.

We wish to explore the idea of labeling antibodies with dirhenium(I) hexacarbonyl units held together by bis(bidentate) ligands such as oxalate. This will enable each antibody molecule to carry a higher payload of radioactive rhenium atoms to the tumour cells, thus enhancing the effectiveness of radioimmunotherapy. A possible way to attach the dirhenium unit to antibodies will be via bifunctional ligands, such as diphosphines which contain carboxyl groups for coupling with the amino groups on antibodies (Fig. 1) [10]. The dirhenium unit is much smaller than a typical antibody molecule, hence it should not interfere with the antibody-epitope recognition if it is conjugated with the antibody away from the epitope-recognition site. We are aware, however, that at the no-carrier-added level, the concentration of mononuclear ^{188}Re precursor currently available [8,9] is too low to favour the formation of dinuclear complexes, and look forward to the future development of efficient methods of concentrating the ^{188}Re precursor.

Herein we report the thermal decarbonylation of $[\{Re(CO)_5\}_2(\mu,\eta^1{:}\eta^1\text{-}C_2O_4)]$ **1** to form the key intermediate $[Re_2(CO)_6(C_2O_4)]_n$, and the representative reactions of the latter with a monophosphine (PPh_3), a non-chelating diphosphine [*trans*-1,2-bis(diphenylphosphino)ethylene (dppene)], and a chelating diphosphine [1,3-bis(diphenylphosphino)propane (dppp)], respectively, to form dirhenium complexes.

2. Results and discussion

2.1. Thermal decarbonylation of complex *1*

Complex **1** is sparingly soluble in most organic solvents, but undergoes thermal decarbonylation to give a product which is soluble in THF. Precipitation with *n*-hexane gives a solid with the empirical formula $[Re_2(CO)_6(C_2O_4)]$. This solid is expected to be polymeric, as shown in Fig. 2, in order that the requirement for an 18-electron octahedral configuration for the Re atoms is satisfied. In THF solution, however, the existence of a solvated monomeric structure, $[Re_2(CO)_6(\mu,\eta^2{:}\eta^2\text{-}C_2O_4)(thf)_2]$, is plausible. The IR spectrum of $[Re_2(CO)_6(C_2O_4)]_n$ in the carbonyl stretching region shows two bands, at 2039 and 1914 cm^{-1}, indicating that the complex contains the tricarbonyl rhenium moiety. The strong band at 1641 cm^{-1} (doublet) and the very weak band at 1347 cm^{-1} are due to the carboxylate stretching, and are consistent with the presence of a bis(bidentate) bridging oxalato group [11,12].

2.2. Reaction of complex *1* with PPh_3

Complex **1** was first refluxed in THF to obtain a solution of $[Re_2(CO)_6(C_2O_4)]_n$. Reaction of the latter with two molar equivalents of PPh_3 in THF gave *anti*-$[Re_2(PPh_3)_2(CO)_6(\mu,\eta^2{:}\eta^2\text{-}C_2O_4)]$ **2**. The thermal decarbonylation step is best carried out before addition of PPh_3, since a small amount of black solid is usually formed when complex **1** is heated. This solid has to be filtered off before PPh_3 is added.

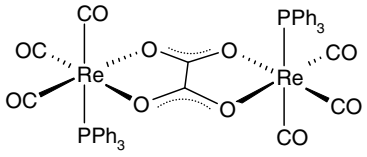

2

The ^{31}P NMR spectrum of **2** shows a single peak at 29.2 ppm, showing that the phosphorus atoms are equivalent. The solution IR spectrum of **2** in the carbonyl stretching region shows three absorption peaks, at 2031, 1937 (sh) and 1909 cm^{-1}, consistent with the presence of $[Re(CO)_3]$ moieties.

Complex **2** is oxidized on prolonged exposure (1 week) of its solution to air, forming the phosphine-oxide complex, *anti*-$[Re_2(OPPh_3)_2(CO)_6(\mu,\eta^2{:}\eta^2\text{-}C_2O_4)]$, **3**. The large cone angle of triphenylphosphine probably results in a weakened bond with Re, which facilitates the

oxidation. Steric hindrance is reduced in the phosphine oxide complex since the {Ph_3P} unit is further removed from the Re atom, and the sp^3 hybridization of the oxygen atom allows the {Ph_3P} unit to bend outwards to avoid steric crowding (Fig. 3). The most obvious spectroscopic indication for the conversion of complex **2** to **3** is the downfield shift of the ^{31}P signal to 45.5 ppm.

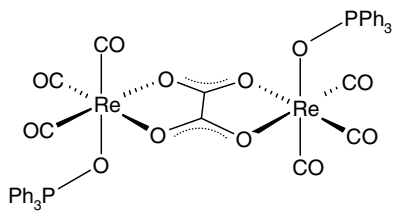

3

2.3. Molecular structure of anti-[$Re_2(OPPh_3)_2(CO)_6(\mu,\eta^2:\eta^2\text{-}C_2O_4)$] 3

The molecule of **3** (Fig. 3) consists of two [$Re(CO)_3(OPPh_3)$] fragments, which are bridged by a tetradentate oxalate ligand. The molecule possesses a crystallographic inversion centre at the midpoint of the C(1)–C(1a) bond of the oxalato bridge. This is the first example, to our knowledge, of a rhenium carbonyl oxalato complex where the oxalato ligand is in the $\mu,\eta^2:\eta^2$-bridging mode, although this coordination mode has been found in many dinuclear oxalato complexes [11,13–20]. The C_2O_4 group is planar, with a maximum deviation of 0.0008 Å [for C(1) and its symmetry-equivalent C(1a)]. The Re atoms lie on opposite sides of the C_2O_4 plane, each deviating significantly (0.45 Å) from the plane. Thus, the [$Re_2C_2O_4$] fragment adopts a chair conformation. The Re–Re separation is 5.608 Å.

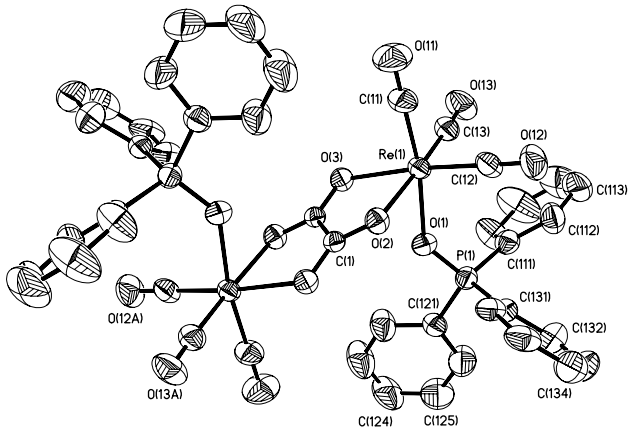

Fig. 3. Molecular structure of *anti*-[$Re_2(OPPh_3)_2(CO)_6(\mu,\eta^2:\eta^2\text{-}C_2O_4)$], **3**.

The three terminal carbonyl groups are in a facial arrangement, such that all CO groups are *trans* to the O-bonded ligands. The {ReO_3C_3} core is a very distorted octahedron and the largest angular distortions are seen in the angles O(3)–Re(1)–O(2) and C(12)–Re(1)–O(1), which are 76.10(6)° and 99.8(3)°, respectively. The average Re–CO bond length is 1.889(8) Å, which is similar to those found for other Re(I) complexes [1,21,22]. The two coordinated $OPPh_3$ ligands adopt an *anti* arrangement. This configuration is expected to be sterically most favourable, since the bulky $OPPh_3$ ligands are as far away from each other as possible.

2.4. Reaction of complex 1 with dppene

Reaction of **1** with dppene in 1:1 molar ratio yields [$Re_2(\mu\text{-dppene})(CO)_6(\mu,\eta^2:\eta^2\text{-}C_2O_4)$] **4** as the only product, the crystal structure of which is discussed below.

Reaction of **1** with two molar equivalents of dppene gave, besides **4**, complex **5**, [$Re_2(\mu\text{-dppene})_2(CO)_6(\mu,\eta^1:\eta^1\text{-}C_2O_4)$]. The ^{31}P NMR spectrum of complex **5** shows only one peak, at 9.4 ppm, indicating that all phosphorus atoms are equivalent. Four peaks in the IR spectrum of complex **5** may be assigned to carboxylate stretching modes (1657, 1629, 1390, and 1261 cm^{-1}). The large frequency difference between the first and last of these peaks ($\Delta = 396$ cm^{-1}) is consistent with the presence of monodentate-coordinated carboxylate groups [12]. The presence of [$Re(CO)_3$] groups is indicated by the positions of the $\nu(C{\equiv}O)$ peaks (2030, 1948, and 1907 cm^{-1}). Elemental analysis and FAB-MS data also agree with the proposed identity of complex **5**.

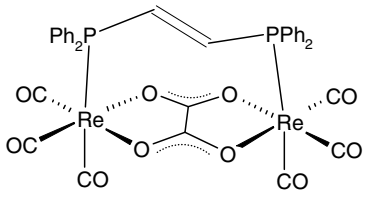

4

A related structure has been crystallographically observed for the complex [$Mo_2(CO)_8(\mu\text{-dppene})_2$] (Fig. 4) [23]. This Mo complex reacts with excess dppene to give the complex [$Mo_2(CO)_6(\mu\text{-dppene})_3$], which, though not

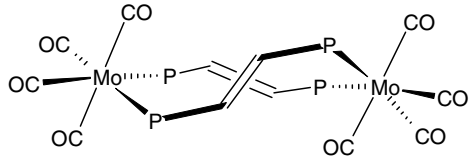

Fig. 4. Molecular structure of [$Mo_2(CO)_8(\mu\text{-dppene})_2$].

characterized by X-ray crystallography, was thought to have three bridging ligands and a *fac*-geometry around each metal, as proposed for complex **5** [23].

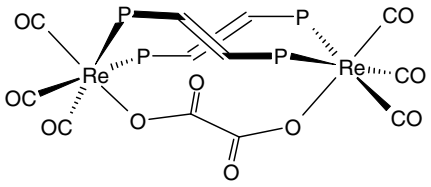

5

2.5. Molecular structure of $[Re_2(\mu\text{-dppene})(CO)_6(\mu,\eta^2{:}\eta^2\text{-}C_2O_4)]$ 4

The structure of complex **4** (Fig. 5) consists of two rhenium atoms bridged by a planar tetradentate oxalate ligand. Each Re atom is also coordinated by three terminal CO groups in facial arrangement.

The C_2O_4 group is practically planar, the maximum deviation being 0.026 Å [for O(1)]. The Re atoms lie on the same side of the C_2O_4 plane, with Re(1) deviating by 0.23 Å from the plane and Re(2) by 0.26 Å. Thus the $\{Re_2C_2O_4\}$ fragment adopts a boat conformation. The average Re–O bond length of **4** (2.176 Å) is slightly longer than that of complex **3** (2.167 Å), while the Re···Re non-bonded distance of 5.613 Å is close to that observed in complex **3** (5.608 Å).

The dppene ligand adopts a "*syn*" conformation wherein the two phosphorus lone pairs of electrons are eclipsed. The atoms Re(1), P(1), P(2), and Re(2) are therefore virtually coplanar, with a maximum deviation of 0.008 Å [for P(2)]. This conformation of dppene, which has not been previously observed, is necessary for the ligand to be able to bridge the two Re atoms held in close proximity by the oxalate bridge. The formation of such an "A-frame" type of bridge by dppene is unexpected since the rigid carbon backbone and *trans* disposition of the phosphorus atoms would favour the "open" bridging mode, where the M–P–C═C–P–M chain is fully extended [23].

The P–CH═CH–P group is not planar, with the two P–C–H fragments being rotated by 17° [the P(1)–C(1)–C(2)–P(2) torsional angle] about the C–C bond. Despite this distortion, which is expected to result in decreased π-overlap between C(1) and C(2), the C(1)–C(2) bond [1.32(1) Å] is shorter than a typical C–C double bond (1.34 Å). The strain in the molecule of **4** is further seen in the elongated Re–P bonds. The average Re–P bond length of 2.502(2) Å is longer than those (ranging from 2.309 to 2.477 Å) found in other Re(I) carbonyl phosphine complexes [2,3,24–28]. The coordination environments of both Re atoms are also severely distorted from the ideal octahedral geometry, as seen from the Re centred bond angles in Table 6. Interestingly, the C(1)–P(1)–Re(1) and C(2)–P(2)–Re(2) angles [108.8(3)° and 111.1(2)°, respectively] are not severely distorted from the theoretical value of 109.5°.

It is interesting to note that, despite the apparent strain in the molecule, complex **4** is formed in very good yield (79%). Moreover, complex **4**, unlike **3**, is stable towards air-oxidation. It would therefore appear that there is a reasonably good fit between dppene (P···P distance 4.471 Å) and the $\{Re_2(\mu,\eta^2{:}\eta^2\text{-}C_2O_4)\}$ unit (Re···Re distance 5.613 Å), and that the potential energy of the Re(I) core is relatively insensitive to distortions from the octahedral coordination geometry.

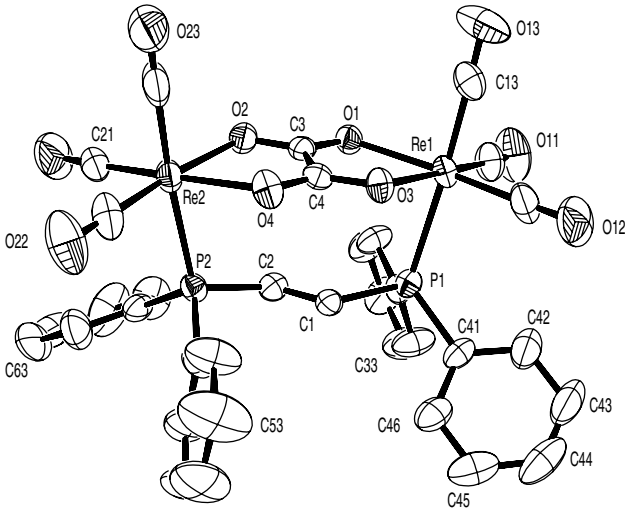

Fig. 5. Molecular structure of $[Re_2(\mu\text{-dppene})(CO)_6(\mu,\eta^2{:}\eta^2\text{-}C_2O_4)]$, **4**.

2.6. Reaction of complex 1 with dppp

In this reaction, the dominant product obtained was $[(\eta^2\text{-dppp})Re(CO)_3(\mu,\eta^1{:}\eta^1\text{-}C_2O_4)Re(CO)_3(\eta^2\text{-dppp})]$ **6** and not $[Re_2(\mu\text{-dppp})(CO)_6(\mu,\eta^2{:}\eta^2\text{-}C_2O_4)]$. Unlike dppene, which is non-chelating due to its rigid backbone, dppp favours the chelating coordination mode, hence compound **6** is preferentially formed.

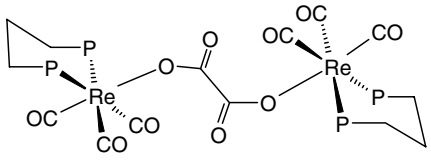

6

The identity of complex **6** was deduced spectroscopically. Three sharp *v*(CO) peaks are observed at 2029, 1949 and 1893 cm^{-1}, which are typical of

$[Re(CO)_3(dppp)]^+$ moieties [29]. In addition, the large difference between the $\nu_{asym}(CO_2)$ and $\nu_{sym}(CO_2)$ frequencies (384 cm^{-1}) is consistent with the monodentate coordination of the carboxyl groups [12]. In the ^{31}P NMR spectrum, only one singlet peak is present, indicating the equivalence of the phosphorus atoms. The ^{31}P chemical shift (−2.5 ppm) is consistent with the chelating mode of dppp [29].

3. Conclusion

The complex $[\{Re(CO)_5\}_2(\mu,\eta^1{:}\eta^1\text{-}C_2O_4)]$ readily undergoes thermal decarbonylation to form $[Re_2(CO)_6(C_2O_4)]_n$. Complexes containing oxalate in the bis(bidentate) $(\mu,\eta^2{:}\eta^2)$ coordination mode are obtained in good yield by reacting $[Re_2(CO)_6(C_2O_4)]_n$ with two equivalents of PPh_3 or one equivalent of *trans*-1,2-bis(diphenylphosphino)ethylene (dppene). Cleavage of two of the Re–O bonds of the $\{Re_2(\mu,\eta^2{:}\eta^2\text{-}C_2O_4)\}$ unit occurs readily in the presence of a chelating diphosphine (dppp) or an excess of a non-chelating diphosphine (dppene). This study also shows that it is possible for dppene to form A-frame complexes, despite its rigid backbone and the *trans* disposition of its phosphorus atoms. Formation of A-frame complexes by dppene is presumably favoured if the two metal atoms in the complex are separated by about 5.6 Å, as in the case of $[Re_2(\mu\text{-dppene})(CO)_6(\mu,\eta^2{:}\eta^2\text{-}C_2O_4)]$. It is therefore potentially interesting to study the functionalization of dppene with carboxyl groups, and the application of the functionalized dppene in the labeling of antibodies with radioactive dirhenium units (Fig. 1). It is also of interest to prepare radioactive $[Re_2(CO)_6(C_2O_4)]_n$ from the well-known precursor $[^{188}Re(CO)_3(H_2O)_3]^+$ [8,9], but our preliminary attempts to prepare $[Re_2(CO)_6(C_2O_4)]_n$ using the non-radioactive model $[ReBr_3(CO)_3]^{2-}$ have not been successful. Another interesting possibility is to prepare $[\{Re(CO)_5\}_2(\mu,\eta^1{:}\eta^1\text{-}C_2O_4)]$ from $[Re(CO)_6][BF_4]$. The use of $[^{188}Re(CO)_6]^+$ as an alternative point of entry into rhenium radiopharmaceutical chemistry has been proposed recently [30].

4. Experimental

4.1. General

All reactions were routinely performed under pure dry nitrogen using standard Schlenk techniques. All solvents for the reactions were also vacuum degassed before use. The solvents were of reagent grade and were purified and dried by published procedures [31]. Chemical reagents, unless otherwise stated, were commercial products and were used without further purification. The complex $[\{Re(CO)_5\}_2(\mu,\eta^1{:}\eta^1\text{-}C_2O_4)]$ **1** was prepared using the reported procedure [4]. Pre-coated silica TLC plates of layer thickness 0.25 mm were purchased from Merck. Fourier transform infrared spectra were recorded with a Perkin–Elmer 1725X FT-IR Spectrometer. Phosphorus-31 NMR spectra were recorded at room temperature on a Bruker DRX400 spectrometer. The phosphorus chemical shifts are quoted from the proton-decoupled spectra, and are reported in ppm to the higher frequency of external 80% H_3PO_4. The fast atom bombardment mass spectrum of **5** was recorded on a VG AutoSpecQ mass spectrometer using a 3-nitrobenzyl alcohol matrix. The mass quoted is that of the (^{185}Re–^{187}Re) ion, which gives the strongest peak in isotope pattern. Elemental analyses were performed using a LECO CHNS-932 instrument.

4.2. Thermal decarbonylation of $[\{Re(CO)_5\}_2(\mu,\eta^1{:}\eta^1\text{-}C_2O_4)]$ 1

Complex **1** (100 mg 0.136 mmol) and distilled THF (20 ml) were placed in a 120-ml Schlenk flask with a stirring bar. The suspension was degassed and filled with nitrogen, then stirred and heated to reflux. The mixture was refluxed for 1 h, during which time most of the solid dissolved, and filtered under nitrogen. The filtrate was concentrated under reduced pressure, and *n*-hexane was then added. The pale yellow precipitate obtained was washed with *n*-hexane several times, and dried under high vacuum to give a solid analysed as $[Re_2(CO)_6(C_2O_4)]_n$. Yield = 75 mg, 88%.

IR (THF)/cm^{-1}: 2029(s) and 1909(vs) ν(C≡O); 1646(s) $\nu(CO_2)$. IR(KBr)/cm^{-1}: 2039(s) and 1914(vs) ν(C≡O); 1641(s) $\nu_{asym}(CO_2)$; 1347 (vw) $\nu_{sym}(CO_2)$. Anal. Calc. for $[C_8O_{10}Re_2]_n$: C, 15.3%. Found: C, 15.2%.

4.3. Reaction of complex 1 with PPh_3

Complex **1** (100 mg 0.136 mmol) and distilled THF (20 ml) were placed in a 120-ml Schlenk flask with a stirring bar. The suspension was degassed and filled with nitrogen, then stirred and heated to reflux. After refluxing for 1 h, the solution was filtered under N_2 to a solution of PPh_3 (71 mg, 0.27 mmol) in 10 ml THF. The resultant mixture was degassed again and then heated at 60 °C for 2 h. The solution was then concentrated to 2–3 ml under reduced pressure and *n*-hexane was added. The white precipitate of *anti*-$[Re_2(PPh_3)_2(CO)_6(\mu,\eta^2{:}\eta^2\text{-}C_2O_4)]$, **2**, formed was isolated by filtration, washed several times with *n*-hexane and recrystallized from CH_2Cl_2–*n*-hexane mixture. Yield = 135 mg, 86%.

IR(CH_2Cl_2)/cm^{-1}: 2031(m), 1937(m, sh) and 1909(vs) ν(C≡O). ^{31}P NMR($CDCl_3$): δ_p 29.2 (singlet). Anal. Calc. for $[C_{44}H_{30}O_{10}P_2Re_2]$: C, 45.8; H, 2.6%. Found: C, 45.5; H, 2.5%.

The complex **2** was oxidized to **3**, *anti*-$[Re_2(OPPh_3)_2(CO)_6(\mu,\eta^2{:}\eta^2\text{-}C_2O_4)]$ on prolonged exposed to air

during the growth of single crystals from CH_2Cl_2–*n*-hexane mixture.

IR(CH_2Cl_2)/cm^{-1}: 2027(m), 1936(w, sh) and 1908(vs) ν(C≡O). IR(KBr)/cm^{-1}: 2026(s) and 1893(vs) ν(C≡O); 1641(s) $\nu_{asym}(CO_2)$; 1346(w) $\nu_{sym}(CO_2)$; 1591(w), 1485(w), 1439(m), 1139(m), 1122(m), 1082(m), 1027(w), 999(w), 913(w), 814(w), 749(w), 727(m), 694(m), 538(m), 510(w). ^{31}P NMR($CDCl_3$): δ_p 45.5 (singlet). Anal. Calc. for [$C_{44}H_{30}O_{12}P_2Re_2$]: C, 44.5; H, 2.5%. Found: C, 44.5; H, 2.6%.

4.4. Reaction of complex *1* with dppene in 1:1 molar ratio

The procedure was similar to that described for the reaction with PPh_3 except for the work-up procedure and that PPh_3 (2×) was replaced by dppene (1×). After the reaction was finished, solvent was evaporated under high vacuum. The residue was dissolved in a minimum quantity of CH_2Cl_2 and applied to silica TLC plates. A dichloromethane–hexane (3:2) mixture eluted a yellow band (R_f = 0.81), from which [Re_2(μ-dppene)-$(CO)_6(\mu,\eta^2{:}\eta^2\text{-}C_2O_4)$], **4**, was recovered by CH_2Cl_2 extraction and recrystallization from CH_2Cl_2–hexane mixture. The yield was 79%.

IR of complex **4** (CH_2Cl_2)/cm^{-1}: 2044(m), 2037(m), 1946(s), 1914(s) ν(C≡O). IR(KBr)/cm^{-1}: 2033(s), 1938(s) and 1913(s) ν(C≡O); 1635(s) $\nu_{asym}(CO_2)$; 1343(w) $\nu_{sym}(CO_2)$; 1484(w), 1437(m), 1262(vw), 1177(w), 1102(w), 1000(vw), 797(w,br), 744(m), 695(m), 524(m). ^{31}P NMR($CDCl_3$): δ_p 33.3 (singlet). Anal. Calc. for [$C_{34}H_{22}O_{10}P_2Re_2$]: C, 39.8; H, 2.1%. Found: C, 38.8; H, 2.1%.

4.5. Reaction of complex *1* with dppene in 1:2 molar ratio

The procedure was similar to that described above except that the molar ratio of complex **1** to dppene was 1:2. A similar work-up procedure gave two bands on the TLC plate: the first band (that of the higher R_f value, 0.81) was identified to be complex **4** [Re_2(μ-dppene)-$(CO)_6(\mu,\eta^2{:}\eta^2\text{-}C_2O_4)$] (21% yield). The second band (R_f = 0.1) was recrystallized by CH_2Cl_2-*n*-hexane mix-

Table 1
Crystal data for *anti*-[$Re_2(OPPh_3)_2(CO)_6(\mu,\eta^2{:}\eta^2\text{-}C_2O_4)$], **3**

Empirical formula	$C_{44}H_{30}O_{12}P_2Re_2$
Formula weight	1185.02
Temperature	293(2) K
Wavelength	0.71073 Å
Crystal system	Triclinic
Space group	$P\bar{1}$
Unit cell dimensions	
a (Å)	9.9097(2)
b (Å)	10.7021(2)
c (Å)	11.0507(2)
α (°)	88.709(1)
β (°)	88.590(1)
γ (°)	68.248(1)
Volume ($Å^3$)	1088.09(4)
Z	1
Density (calculated) (Mg/m^3)	1.808
Absorption coefficient (mm^{-1})	5.692
F(000)	570
Crystal size	0.12×0.11×0.06 mm^3
Θ range for data collection (°)	2.05–29.26
Reflections collected	8233
Independent reflections	5142 [*R*(int) = 0.0294]
Absorption correction	SADABS
Max. and min. transmission	0.694587 and 0.480958
Data/restraints/parameters	5142/0/271
Final *R* indices [$I > 2\sigma(I)$]	R_1 = 0.0450, wR_2 = 0.0871
R indices (all data)	R_1 = 0.0654, wR_2 = 0.0972
Largest diff. peak and hole (e $Å^{-3}$)	1.494 and −1.175

Table 2
Selected bond lengths [Å] for *anti*-[$Re_2(OPPh_3)_2(CO)_6(\mu,\eta^2{:}\eta^2\text{-}C_2O_4)$], **3**

Re(1)–C(11)	1.900(7)
Re(1)–C(12)	1.879(8)
Re(1)–C(13)	1.887(8)
Re(1)–O(1)	2.150(4)
Re(1)–O(2)	2.173(4)
Re(1)–O(3)	2.162(4)
P(1)–O(1)	1.505(5)
P(1)–C(111)	1.799(8)
P(1)–C(121)	1.798(7)
P(1)–C(131)	1.790(7)
O(2)–C(1)	1.253(7)
O(3)–C(1a)	1.258(7)
C(1)–C(1a)	1.54(1)

Table 3
Selected bond angles [°] for *anti*-[$Re_2(OPPh_3)_2(CO)_6(\mu,\eta^2{:}\eta^2\text{-}C_2O_4)$], **3**

C(11)–Re(1)–O(1)	170.9(3)
C(11)–Re(1)–O(2)	95.8(3)
C(11)–Re(1)–O(3)	95.8(3)
C(12)–Re(1)–C(11)	87.3(3)
C(12)–Re(1)–C(13)	88.7(3)
C(12)–Re(1)–O(1)	99.8(3)
C(12)–Re(1)–O(2)	98.3(3)
C(12)–Re(1)–O(3)	173.9(2)
C(13)–Re(1)–C(11)	87.8(3)
C(13)–Re(1)–O(1)	98.0(3)
C(13)–Re(1)–O(2)	172.2(2)
C(13)–Re(1)–O(3)	96.7(2)
O(1)–Re(1)–O(2)	77.5(2)
O(1)–Re(1)–O(3)	76.7(2)
O(3)–Re(1)–O(2)	76.1(2)
C(1)–O(2)–Re(1)	113.2(4)
C(1a)–O(3)–Re(1)	114.1(4)
O(2)–C(1)–C(1a)	117.4(7)
O(3a)–C(1a)–C(1)	116.0(6)
P(1)–O(1)–Re(1)	137.0(3)
O(1)–P(1)–C(111)	111.9(3)
O(1)–P(1)–C(121)	107.2(3)
O(1)–P(1)–C(131)	110.5(3)
C(121)–P(1)–C(111)	108.2(3)
C(131)–P(1)–C(111)	109.2(3)
C(131)–P(1)–C(121)	109.7(3)

Table 4
Crystal data for $[Re_2(\mu\text{-dppene})(CO)_6(\mu,\eta^2{:}\eta^2\text{-}C_2O_4)]$, **4**

Empirical formula	$C_{34}H_{22}O_{10}P_2Re_2$
Formula weight	1024.86
Temperature (K)	298(2)
Wavelength (Å)	0.71073
Crystal system	Monoclinic
Space group	*P*2(1)/*c*
Unit cell dimensions	
a (Å)	12.22(1)
b (Å)	20.792(6)
c (Å)	14.428(3)
α (°)	90
β (°)	109.85(5)
γ (°)	90
Volume (Å^3)	3447(4)
Z	4
Density (calculated) (Mg/m^3)	1.975
Absorption coefficient (mm^{-1})	7.165
F(000)	1944
Crystal size (mm^3)	0.2×0.5×0.5
Θ range for data collection (°)	1.77–27.50
Reflections collected	9494
Independent reflections	7906 [*R*(int)=0.0355]
Absorption correction	Semi-empirical from psi-scans
Max. and min. transmission	0.6621 and 0.3780
Data/restraints/parameters	7098/0/433
Final *R* indices [$I>2\sigma(I)$]	$R_1=0.0472$, $wR_2=0.0904$
R indices (all data)	$R_1=0.0873$, $wR_2=0.1120$
Largest diff. peak and hole (e Å^{-3})	1.364 and −1.043

ture to give a white powder, identified to be $[Re_2(\mu\text{-dppene})_2(CO)_6(\mu,\eta^1{:}\eta^1\text{-}C_2O_4)]$, **5**. The yield was 30%.

IR of complex **5** (CH_2Cl_2)/cm^{-1}: 2036(vs), 1958(s), 1910(s) *v*(C≡O). IR(KBr)/cm^{-1}: 2030(vs), 1948(s), 1907(s) *v*(C≡O); 1657(m), 1629(m), 1390(w), 1261(m) *v*(CO_2); 1743(w), 1483(w), 1436(m), 1093(w), 745(m), 697(m). ^{31}P NMR($CDCl_3$): δ_p 9.4 (singlet). Anal. Calc. for $C_{60}H_{44}O_{10}P_4Re_2$: C, 50.7; H, 3.1%. Found: C, 49.3; H, 3.3%. FAB-MS: *m*/*z* 1423([M + 2H]).

Table 5
Selected bond lengths [Å] for $[Re_2(\mu\text{-dppene})(CO)_6(\mu,\eta^2{:}\eta^2\text{-}C_2O_4)]$, **4**

Re(1)–C(11)	1.896(9)
Re(1)–C(12)	1.892(9)
Re(1)–C(13)	1.91(1)
Re(1)–O(1)	2.181(5)
Re(1)–O(3)	2.176(5)
Re(1)–P(1)	2.511(2)
Re(2)–C(21)	1.90 (1)
Re(2)–C(22)	1.87(1)
Re(2)–C(23)	1.94(1)
Re(2)–O(2)	2.171(6)
Re(2)–O(4)	2.178(5)
Re(2)–P(2)	2.493(2)
P(1)–C(1)	1.806(8)
P(2)–C(2)	1.807(8)
C(1)–C(2)	1.32(1)
C(3)–C(4)	1.54(1)
C(3)–O(1)	1.244(9)
C(3)–O(2)	1.248(9)
C(4)–O(3)	1.246(9)
C(4)–O(4)	1.245(9)

4.6. Reaction of complex *1* with dppp in 1:1 molar ratio

The procedure was similar to that described above except that dppene was replaced by dppp. Separation by TLC using a CH_2Cl_2–*n*-hexane (3:2) mixture as eluant gave a main colourless band (R_f=0.74), from which $[(\eta^2\text{-dppp})Re(CO)_3(\mu,\eta^1{:}\eta^1\text{-}C_2O_4)Re(CO)_3(\eta^2\text{-dppp})]$ **6** was obtained by acetone extraction and recrystallization from CH_2Cl_2–*n*-hexane mixture. The yield was 19%.

IR of complex **6** (KBr)/cm^{-1}: 2029 (s), 1949 (s), 1892 (vs) *v*(C≡O); 1646 (s) $v_{asym}(CO_2)$; 1261 (s) $v_{sym}(CO_2)$. ^{31}P NMR ($CDCl_3$): δ_p −2.5 ppm (singlet). Anal. Calc. for $C_{62}H_{52}O_{10}P_4Re_2$: C, 51.2; H, 3.6%. Found: C, 51.8; H, 5.6%.

Table 6
Selected bond angles [°] for $[Re_2(\mu\text{-dppene})(CO)_6(\mu,\eta^2{:}\eta^2\text{-}C_2O_4)]$, **4**

C(11)–Re(1)–C(12)	90.9(4)
C(11)–Re(1)–C(13)	89.0(4)
C(12)–Re(1)–C(13)	89.5(4)
C(11)–Re(1)–O(1)	98.9(3)
C(11)–Re(1)–O(3)	174.1(3)
C(11)–Re(1)–P(1)	90.3(3)
C(12)–Re(1)–O(1)	170.2(3)
C(12)–Re(1)–O(3)	94.4(3)
C(12)–Re(1)–P(1)	94.0(3)
C(13)–Re(1)–O(1)	90.8(3)
C(13)–Re(1)–O(3)	93.7(3)
C(13)–Re(1)–P(1)	176.3(3)
O(3)–Re(1)–O(1)	75.8(2)
O(1)–Re(1)–P(1)	85.8(2)
O(3)–Re(1)–P(1)	86.7(2)
C(21)–Re(2)–C(22)	88.5(4)
C(21)–Re(2)–C(23)	92.4(5)
C(22)–Re(2)–C(23)	90.8(5)
C(21)–Re(2)–O(2)	96.4(3)
C(21)–Re(2)–O(4)	171.9(3)
C(21)–Re(2)–P(2)	91.5(3)
C(22)–Re(2)–O(2)	174.4(3)
C(22)–Re(2)–O(4)	99.0(3)
C(22)–Re(2)–P(2)	91.0(3)
C(23)–Re(2)–O(2)	91.7(4)
C(23)–Re(2)–O(4)	90.7(4)
C(23)–Re(2)–P(2)	175.8(3)
O(2)–Re(2)–O(4)	75.9(2)
O(2)–Re(2)–P(2)	86.3(2)
O(4)–Re(2)–P(2)	85.3(2)
C(1)–P(1)–Re(1)	108.8(3)
C(2)–P(2)–Re(2)	111.1(2)
C(1)–C(2)–P(2)	123.1(6)
C(2)–C(1)–P(1)	126.1(6)
O(1)–C(3)–O(2)	125.8(7)
O(1)–C(3)–C(4)	117.5(6)
O(2)–C(3)–C(4)	116.7(7)
O(3)–C(4)–C(3)	117.1(7)
O(4)–C(4)–C(3)	117.7(6)
O(4)–C(4)–O(3)	125.2(7)
C(3)–O(1)–Re(1)	114.3(5)
C(3)–O(2)–Re(2)	114.6(5)
C(4)–O(3)–Re(1)	114.5(5)
C(4)–O(4)–Re(2)	114.0(5)

4.7. Crystallography

X-ray-quality single crystals of both **3** and **4** were grown from CH_2Cl_2-*n*-hexane mixture at ca. 5 °C.

Crystals were mounted on quartz fibres (**4**) or sealed in glass capillary (**3**). For complex **3**, X-ray data were collected at 295(2) K on a Siemens SMART diffractometer equipped with a CCD detector, using graphite-monochromated Mo Kα radiation ($\lambda = 0.71073$ Å). Data were corrected for Lorentz and polarisation effects with the SMART suite of programs [32], and for absorption effects with SADABS [33].

For complex **4**, X-ray data were collected at 298(2) K by $\theta/2\theta$ scan using a Siemens P4 diffractometer with graphite-monochromated Mo Kα radiation. Absorption corrections were performed using psi-scan data.

Crystal structures were solved by direct methods and refined using full-matrix least-squares on F^2 using the SHELXTL suite of programs [34]. Hydrogen atoms were placed in calculated positions and given isotropic thermal parameters at 1.2 times those of the C atoms to which they are attached. All non-hydrogen atoms were given anisotropic displacement parameters in the final model.

Crystallographic data for **3** and **4** are summarized in Tables 1 and 4, respectively. Selected bond lengths and angles are listed in Tables 2 and 3 (for **3**) and Tables 5 and 6 (for **4**), respectively.

5. Supplementary material

Crystallographic data (excluding structure factors) for the structures reported in this paper have been deposited with the Cambridge Crystallographic Data Centre as supplementary publications nos. CCDC 239509 (complex **3**) and 239510 (complex **4**). Copies of the data can be obtained free of charge on application to CCDC, 12 Union Road, Cambridge CB2 1EZ, UK (fax: +44-1223-336-033; e-mail: deposit@ccdc.cam.ac.uk or www: http://www.ccdc.cam.ac.uk).

Acknowledgement

We acknowledge the financial support (Grant No. RP 23/98 YYK) of the National Institute of Education, Nanyang Technological University (NTU). Rui Zhang and Chee Leong Kee are grateful to the NTU for scholarship awards.

References

[1] F.A. Cotton, E.V. Dikarev, M.A. Petrukhina, Inorg. Chim. Acta 284 (1999) 304.
[2] G. La Monica, S. Cenini, E. Forni, M. Manassero, V.G. Albano, J. Organomet. Chem. 112 (1976) 297.
[3] C.J. Cameron, P.E. Fanwick, M. Leeaphon, R.A. Walton, Inorg. Chem. 28 (1989) 1101.
[4] K. Raab, W. Beck, Chem. Ber. 118 (1985) 3830.
[5] E. Linder, R. Grimmer, J. Organomet. Chem. 31 (1971) 249.
[6] J.R. Dilworth, S.J. Parrott, Chem. Soc. Rev. 27 (1998) 43.
[7] D.E. Reichert, J.S. Lewis, C.J. Anderson, Coord. Chem. Rev. 184 (1999) 3.
[8] R. Alberto, R. Schibli, R. Waibel, U. Abram, A.P. Schubiger, Coord. Chem. Rev. 190–192 (1999) 901.
[9] R. Alberto, R. Schibli, A. Egli, A.P. Schubiger, U. Abram, T.A. Kaden, J. Am. Chem. Soc. 120 (1998) 7987.
[10] J. Zhang, J.J. Vittal, W. Henderson, J.R. Wheaton, I.H. Hall, T.S.A. Hor, Y.K. Yan, J. Organomet. Chem. 650 (2002) 123.
[11] K.L. Scott, K. Wieghardt, A.G. Sykes, Inorg. Chem. 12 (1973) 655.
[12] G.B. Deacon, R.J. Philips, Coord. Chem. Rev. 33 (1980) 27.
[13] R. Weinland, F. Paul, Z. Anorg. Allg. Chem. 129 (1923) 243.
[14] J. Chatt, F.G. Mann, A.F. Wells, J. Chem. Soc. (1938) 2086.
[15] N.F. Curtis, J. Chem. Soc. (1963) 4109.
[16] N.F. Curtis, J. Chem. Soc. A (1968) 1548.
[17] J. Garaji, Chem. Commun. (1968) 904.
[18] N.W. Alcock, Chem. Commun. (1968) 1327.
[19] M.G.B. Drew, G.W.A. Fowles, D.F. Lewis, Chem. Commun. (1969) 876.
[20] P.-T. Cheng, B.R. Loescher, S.C. Nyburg, Inorg. Chem. 10 (1971) 1275.
[21] S.M. Woessner, J.B. Helms, Yibing Shen, B.P. Sullivan, Inorg. Chem. 37 (1998) 5406.
[22] S. Trammell, P.A. Goodson, B.P. Sullivan, Inorg. Chem. 35 (1996) 1421 and references therein.
[23] G.B. Jacobsen, B.L. Shaw, M. Thornton-Pett, J. Organomet. Chem. 323 (1987) 313.
[24] V.G. Albano, P.L. Bellon, G. Ciani, J. Organomet. Chem. 31 (1971) 75.
[25] B.R. Davies, J.A. Ibers, Inorg. Chem. 10 (1971) 578.
[26] Y. Wang, Y. Gao, Q. Shi, Polyhedron 11 (1992) 2483.
[27] S.K. Mandal, D.M. Ho, M. Orchin, Polyhedron 17 (1998) 607.
[28] D.R. Derringer, P.E. Fanwick, R.A. Walton, Inorg. Chem. 28 (1989) 1384.
[29] K. Johnson, T. Frazier, T.M. Becker, K. Miller, D.G. Ho, J. Krause-Bauer, S.K. Mandal, Inorg. Chem. Commun. 4 (2001) 602.
[30] S. Masi, S. Top, S. Dagorne, R. Welter, G. Jaouen, J. Organomet. Chem. 689 (2004) 273.
[31] A.J. Gordon, R.A. Ford, The Chemist's Companion: A Handbook of Practical Data, Techniques and References, Wiley-Interscience, New York, 1972.
[32] SMART Software Reference Manual, Version 4.0, Siemens Energy & Automation, Inc., Analytical Instrumentation, Madison, WI, 1996.
[33] G.M. Sheldrick, SADABS, a Software for Empirical Absorption Correction, University of Göttingen, 1996.
[34] SHELXTL Reference Manual, Version 5.03, Siemens Energy & Automation, Inc., Analytical Instrumentation, Madison, WI, 1996.